

Original Research

Elucidating the Pathogenic Mechanism of Spinal Muscular Atrophy Through the Investigation of *UTS2*

Xu Zhang^{1,2}, Liqi Yang^{1,*}

Academic Editor: Alika K. Maunakea

Submitted: 14 November 2024 Revised: 12 December 2024 Accepted: 25 December 2024 Published: 20 February 2025

Abstract

Background: Spinal muscular atrophy (SMA) is a severe neuromuscular disorder caused by mutations in the survival motor neuron 1 (SMNI) gene, resulting in progressive motor neuron loss and muscle atrophy. The urotensin 2 (UTS2) gene, located on chromosome 9q34.2, plays a significant role in cellular activities such as proliferation, apoptosis, and inflammatory responses. Notably, elevated expression levels of UTS2 have been observed in SMA patients. However, its precise contribution to disease pathogenesis remains unclear. This study aimed to investigate the effects of UTS2, which is overexpressed in SMA patients, in SMA cell models using a UTS2 inhibitor. Methods: We conducted genomic sequencing and bioinformatics analysis on clinical samples to identify proteins highly expressed in association with SMA. Using RNA interference technology, we suppressed SMNI gene expression in bone marrow mesenchymal stem cells (MSCs) to establish an in vitro cellular model of SMA. To assess the biological consequences of SMNI gene knockdown, we employed molecular biological techniques such as immunofluorescence, reverse transcription quantitative polymerase chain reaction (RT-qPCR), and western blotting. Furthermore, we treated the SMA cellular model with the urantide UTS2 receptor inhibitor and examined its effects on cell proliferation, apoptosis, and the expression of relevant proteins. Results: UTS2 was successfully identified as a highly expressed protein associated with SMA. A stable MSC model with SMNI gene knockdown was established. RNA interference (RNAi) technology effectively suppressed SMN1 gene expression, leading to changes in cellular morphology and neuronspecific marker expression. Urantide intervention significantly affected both proliferation and apoptosis in the SMA cell model in a dose-dependent manner. Techniques such as the 3-(4,5-dimethylthiazol-2-yl)-2,5-diphenyltetrazolium bromide (MTT) assay, TUNEL fluorescence staining, and flow cytometry analysis revealed that uride decreased cell viability while increasing the proportion of apoptotic cells. Following urantide intervention, there was a notable increase in caspase-3 messenger ribonucleic acid (mRNA) levels, as well as an increase in caspase-3 protein expression, as demonstrated by immunofluorescence analysis. Conclusion: We elucidated the role of the UTS2 gene in an SMA cell model, emphasizing its dysregulation and identifying potential therapeutic targets. Urantide, a UTS2 inhibitor, had significant biological effects on the SMA cell model, indicating that it is a promising therapeutic strategy for SMA. These findings provide valuable insights for advancing drug development and clinical treatment of SMA.

Keywords: spinal muscular atrophy; RNAi; UTS2; urantide; Caspase-3

1. Introduction

Spinal muscular atrophy (SMA) is a prevalent genetic neurodegenerative disorder that primarily affects pediatric populations and is characterized by the progressive degeneration of motor neurons, leading to muscle weakness and atrophy. The incidence rate of SMA is approximately 1 in 10,000 individuals [1-3], with a carrier frequency of 1 in 250 individuals [2]. The genetic basis of SMA primarily involves the deletion or mutation of exon 7 in the SMN1 gene. Although the survival motor neuron 2 (SMN2) gene shares a similar sequence with SMN1, it predominantly produces an incompletely functional SMN protein that cannot fully compensate for the loss of SMN1 [4,5]. A reduction in SMN protein levels plays a pivotal role in the survival and functionality of motor neurons, and its depletion leads to alpha motor neuron degeneration, muscle atrophy, and activation of the Caspase3-mediated cell apoptosis pathway [5]. Moreover, the SMN protein performs critical regulatory functions within the nucleus by participating in small nuclear ribonucleoprotein (snRNP) biosynthesis and messenger ribonucleic acid (mRNA) splicing processes that are vital for neuronal viability. Insufficient levels of SMN protein result in RNA metabolism disorders and subsequent cellular death, ultimately manifesting as clinical symptoms observed in SMA [6,7].

The impact of SMAs on patients' quality of life is significant, and current treatment options are limited. Despite the approval of certain gene therapies and small-molecule drugs, a definitive cure for SMA has yet to be achieved [8,9]. Furthermore, these drugs, such as nusinersen and risdiplam, which function by promoting the inclusion of exon 7 in the *SMN* pre-mRNA, primarily target SMN itself [9,10]. Research focusing on downstream genes affected by SMN and drug development in this area is scarce, highlighting the urgent need to address specific gene expression regulation and identify potential therapeutic targets [3,9].

¹Department of Pediatrics, The Second Affiliated Hospital of Anhui Medical University, 230601 Hefei, Anhui, China

²Department of Pediatrics, Fuyang People's Hospital, 236000 Fuyang, Anhui, China

^{*}Correspondence: yangliqi0824@163.com (Liqi Yang)

Located on chromosome 9q34.2, urotensin 2 (UTS2) is a member of the urotensin II-related peptide (UII) family, which is involved in various physiological processes, including promoting cell proliferation [11], inhibiting apoptosis [12], and inhibiting the inflammatory response [13]. In the context of SMA, UTS2 expression levels are significantly elevated, suggesting a possible contribution to disease progression [13]. The precise mechanisms by which UTS2 influences SMA pathology are not yet fully understood, but several hypotheses have been proposed. One line of thought is that UTS2 may exacerbate motor neuron degeneration by promoting cell death pathways or disrupting neuromuscular junctions, which are critical for motor neuron function [14]. Additionally, UTS2 could interact with other cellular components affected by SMN deficiency, thereby modulating the cellular response to SMN loss. Despite the growing interest in UTS2, research in this area is still in its infancy. Most studies to date have focused on characterizing UTS2 expression patterns in SMA patients and correlating these findings with disease severity [11,13,14]. Few studies have investigated the functional implications of UTS2 upregulation in SMAs [15,16], and even fewer have explored the therapeutic potential of targeting UTS2. This gap in knowledge underscores the need for more in-depth investigations into the role of UTS2 in SMAs, particularly in terms of its downstream effects on cellular processes and its potential as a therapeutic intervention.

The objective of this study was to elucidate the pathogenic mechanism underlying SMA through clinical sample analysis and *in vitro* experiments. Gene chip analysis and bioinformatics methods revealed that the highly expressed protein UTS2 was associated with SMA. RNA interference technology can be employed to inhibit the expression of the *SMN1* gene in mesenchymal stem cells (MSCs), thereby establishing an SMA cell model. The ultimate aim of this study was to investigate whether inhibitors targeting UTS2 proteins can effectively reverse the disease phenotype in SMA cells, thus providing novel therapeutic strategies for the clinical management of SMA.

2. Materials and Methods

2.1 Participants

The study was approved by the Fuyang People's Hospital ethics committee (approval number: [2024]64), and all participants or their families/legal guardians provided informed consent in accordance with the ethical standards of the Helsinki declaration.

In this study, we recruited a cohort of patients diagnosed with SMA (n = 5) and matched healthy controls (n = 5) from Fuyang People's Hospital between January 2024 and June 2024. The inclusion criteria for participant selection were as follows: (1) met the clinical diagnostic criteria for SMA [17] and (2) had a homozygous deletion of the *SMN1* gene detected [4]. The inclusion criterion for

the normal control group was a copy number of 2 for the *SMN1* gene. The exclusion criteria for participant selection were as follows: (1) the presence of blood disorders; (2) the presence of bone tumors; (3) treatment that could influence SMA progression or symptoms, such as ongoing gene therapy or pharmacological interventions; (4) a history of other neuronuscular disorders that could confound the results; and (5) a family history of genetic disorders that might affect the interpretation of genetic data related to the SMA.

2.2 Observational Indicators

(1) Motor function assessments: Motor function was evaluated via standardized scales to measure muscle strength, coordination, and motor milestones in SMA patients. (2) Neurophysiological measurements: Electromyography (EMG) and nerve conduction studies were performed to assess the functional integrity of motor neurons and neuromuscular junctions. (3) Biochemical markers: The levels of UTS2 and other relevant proteins in the blood and spinal fluid were quantified to correlate with disease severity and response to treatment. (4) Imaging studies: Neuroimaging techniques, such as magnetic resonance imaging (MRI), have been employed to monitor changes in muscle and neuronal structure, providing insights into disease progression. (5) Histopathological examination: Tissue biopsies, when available, were examined for signs of muscle degeneration, neuronal loss, and other pathological features associated with the SMA. (6) Molecular and Cellular Analysis: The expression levels of UTS2 and related genes in patient-derived cells were analyzed to understand the underlying molecular mechanisms.

2.3 RNA-seq Analysis

To obtain differential expression gene information, total RNA was extracted from peripheral blood samples collected from the antecubital vein of the participants. The collection process involved the use of sterile vacutainer tubes containing an appropriate anticoagulant, such as EDTA, to prevent blood clotting. Once collected, the samples were gently inverted several times to ensure thorough mixing with the anticoagulant and then stored on ice.

The total peripheral blood RNA was then extracted via TRIzol Reagent, a monophasic solution of phenol and guanidine isothiocyanate that effectively lyses cells and inactivates RNases, thus preserving the integrity of the RNA. Following extraction, the purity, concentration, and integrity of the RNA were assessed via a combination of NanoDrop (Thermo Fisher Scientific, Waltham, MA, USA) and Agilent 2100/4200 systems (Agilent Technologies, Santa Clara, CA, USA). The NanoDrop provides a rapid and accurate measurement of RNA concentration and purity by determining the absorbance at 260 nm and 280 nm, whereas the Agilent 2100/4200 systems offer a detailed electropherogram that assesses RNA integrity through the analysis of ribosomal RNA peaks.



After assessment, the RNA samples were aliquoted into RNase-free tubes and stored at $-80\,^{\circ}\text{C}$ until further use. This low-temperature storage ensures the long-term preservation of RNA integrity, preventing degradation that could occur due to RNase activity or other environmental factors.

Subsequently, 3 µg of RNA was subjected to mRNA enrichment, fragmentation, and complementary DNA (cDNA) synthesis. The cDNA was processed through endrepair, A-tailing, and purification via Hieff NGS® DNA Selection Beads (Yeasen, Shanghai, China). The purified cDNA was amplified to form single-stranded circular DNA (ss-cDNA), which was then transformed into DNA nanoballs (DNBs) through rolling circle amplification (RCA). The final library was quantified with a Qubit (Thermo Fisher Scientific, Waltham, MA, USA) to confirm adequate sequencing input.

2.4 Sequencing and Service Provider

The RNA-seq library was sequenced on the DNBSEQ-T7 platform with a PE150 model, leveraging the high-throughput capabilities of next-generation sequencing. This service was provided by Bioyi Biotechnology Co., Ltd. (Wuhan, Hubei, China), ensuring the generation of high-quality paired-end reads for comprehensive transcriptome analysis.

2.5 Bioinformatics Analysis

To gain insight into the biological functions and pathways associated with these differentially expressed genes (DEGs), Gene Ontology (GO) and Kyoto Encyclopedia of Genes and Genomes (KEGG) enrichment analyses were performed. In the quality control process, the raw sequencing reads were first processed via fastp software 0.21.0 (SB-Grid Consortium, Cambridge, MA, USA) to remove lowquality data, including 3' end sequences containing adapters and reads with an average quality score below Q20, ensuring that only high-quality reads were used for subsequent analysis. These high-quality reads were subsequently aligned to a reference genome via HISAT2 software 2.1.0 (Center for Computational Biology at Johns Hopkins University, Baltimore, MD, USA). For gene expression analysis, String Tie software 2.1.5 (Center for Computational Biology at Johns Hopkins University, Baltimore, MD, USA) was used to quantify gene expression levels, which were normalized to fragments per kilobase of transcript per million mapped reads (FPKM). Furthermore, DESeq2 software 1.30.1 (Bioconductor Project, Dortmund, Germany) was used to identify DEGs on the basis of the criteria of $|\log 2$ FoldChange| > 1 and $p \le 0.05$. To correct for multiple comparisons in gene expression and enrichment analyses, we employed a false discovery rate (FDR) control method. Specifically, we used the Benjamini-Hochberg procedure [18] to adjust the p values, setting the significance threshold at an FDR of 0.01 for gene expression analysis and an FDR of 0.05 for GO and KEGG enrichment analyses. This

approach helps to control the expected proportion of false positives among the significant results, ensuring the robustness and reliability of our findings.

Finally, to investigate the enrichment of differentially expressed genes in biological functions and pathways, Cluster Profiler software 3.18.1 (Bioconductor Project, Dortmund, Germany) was used for Gene Ontology (GO) and Kyoto Encyclopedia of Genes and Genomes (KEGG) enrichment analyses. Significance was defined as $p \leq 0.05$. We used the abovementioned FDR control method to correct for multiple comparisons in these analyses.

2.6 Cell Isolation and Culture

Human bone marrow mesenchymal stem cells (hBM-MSCs) were isolated from healthy donors via a sterile procedure, which typically involves the following steps: bone marrow aspiration under aseptic conditions, density gradient centrifugation to enrich the MSC population, initial plastic adherence to select for MSCs, and subsequent culture expansion in a sterile incubator while monitoring for cell confluence and viability, ensuring that the entire process adheres to good manufacturing practice (GMP) standards to maintain sterility and cell purity. The bone marrow was flushed with L-DMEM (Gibco, #11885084, Thermo Fisher Scientific, Waltham, MA, USA) supplemented with 10% FBS (Gibco, #10082147, Thermo Fisher Scientific, Waltham, MA, USA) to create a cell suspension, which was then centrifuged at 1500 rpm for 10 minutes to remove the adipose tissue and supernatant. The resulting cell pellet was resuspended in fresh L-DMEM and homogenized by gentle pipetting. Mononuclear cells were separated via lymphocyte separation medium (density of 1.077 g/mL), washed twice, counted, and plated at a density of 1×10^6 cells/mL in culture flasks containing 5 mL of culture medium, resulting in hBM-MSCs.

hBM-MSCs were cultured in low-glucose complete DMEM (BL301A, Pricella, Shanghai, China) and maintained at 37 °C in a humidified atmosphere containing 5% CO₂, and the medium was subsequently changed every 3–4 days. All cell lines were validated by short tandem repeat (STR) profiling and tested negative for mycoplasma.

2.7 RNA Interference and Construction of the SMA Cell Model

The experimental design included several groups to evaluate the impact of short hairpin RNA (shRNA)-mediated *SMNI* knockdown and the subsequent effects of *UTS2* inhibition with urantide on human bone marrow mesenchymal stem cells (hBM-MSCs). The groups included a time point group transfected with *SMNI*-targeting shRNA at the beginning (0 h), a group assessed 48 hours posttransfection, a nontargeting shRNA control group (pshRNA-0), and an *SMNI* shRNA treatment group (pshRNA-*SMNI*). Additionally, a baseline control group of untransfected cells was included, alongside an SMA cell model group



(SMA), and two groups were treated with low (10 nM, L-Urantide+SMA) and high (20 nM, H-Urantide+SMA) concentrations of uranide.

For transfection, hBM-MSCs were plated in 24-well plates at a density of 50,000 cells per well and allowed to adhere overnight under cell culture conditions at 37 °C and 5% CO₂. The following day, the cells were transfected with the recombinant pLKO.1-shRNA plasmids via Lipofectamine 3000 (#L3000008, Thermo Fisher Scientific, Waltham, MA, USA) in Opti-MEM (#31985062, Thermo Fisher Scientific, Waltham, MA, USA) reduced serum medium following the manufacturer's instructions. The DNA-Lipofectamine complexes were added to the cells, which were subsequently incubated for 6 hours to facilitate complex formation and uptake, after which the medium was replaced with fresh complete growth medium. After a 48-hour incubation to allow for gene silencing, the cells were harvested for analysis, such as reverse transcription quantitative polymerase chain reaction (RT-qPCR). Western blot analysis, immunofluorescence staining and cell viability and apoptosis assays.

The efficiency of SMN1 knockdown was determined by quantifying the expression of SMN1 mRNA via reverse transcription quantitative polymerase chain reaction (RTqPCR), and the results were normalized to those of the housekeeping gene GAPDH to determine relative expression levels. The shRNA sequences used were as follows: SMN-shRNA-1F-ATAGTATACGAAAATAGTCACTT CAAGAGAGTGACTATTTTCGTATACTAT, SMN-sh RNA-1R-GACTATTTTCGTATACTATTTAAGTTCTC TAAATAGTATACGAAAATAGTC, SMN-shRNA-2F-AAATAGTATACGAAAATAGTCTTCAAGAGAGACT ATTTTCGTATACTATTT, SMN-shRNA-2R-CTATTTT CGTATACTATTTCGAAGTTCTCTCGAAATAGTATA CGAAAATAG, SMN-shRNA-3F-TGTAAACAGGGGT TGAAAGGTTTCAAGAGAACCTTTCAACCCCTGTT TACA, SMN-shRNA-3R-CTTTCAACCCCTGTTTACA AGAAGTTCTCTTGTAAACAGGGGTTGAAAG, sh -NC-F-CACCGTTCTCCGAACGTGTCACGTTTCAAG AGAACGTGACACGTTCGGAGAATTTTTTG, sh-NC-F-GATCCAAAAAATTCTCCGAACGTGTCACGTTCT CTTGAAACGTGACACGTTCGGAGAAC.

2.8 Real-time Quantitative PCR (RT-qPCR)

Total RNA was extracted from cells via the Cell/Tissue Total RNA Isolation Kit V2 (Vazyme, Nanjing, Jiansu, China). The HiScript lll 1st Strand cDNA Synthesis Kit (Vazyme, China) was used to synthesize cDNA, followed by RT-qPCR using Taq Pro Universal SYBR qPCR Master Mix (Vazyme, China). The relative expression levels of *fl-SMN* mRNA were calculated via the $2^{-\Delta\Delta Ct}$ method, with *GAPDH* serving as the endogenous control. The primers used were as follows: SMN-F-CCAC TTACTATCATGCTGGCTG, SMN-R-CCACTTACTAT CATGCTGGCTG, Caspase-3-F-TGCTATTGTGAGGCG

GTTGT, Caspase-3-R-TCACGGCCTGGGATTTCAAG, GAPDH-F-ACCACAGTCCATGCCATCAC, and GAPD H-R-TCCACCACCCTGTTGCTGTA.

2.9 Western Blot Analysis

Protein extraction was performed via RIPA lysis buffer (Beyotime, Shanghai, China) supplemented with PMSF (Beyotime, China). Protein concentrations were determined via a BCA protein assay kit (NCM Biotech, Nanjing, Jiangsu, China). Equal amounts of protein were separated by SDS-PAGE and transferred onto PVDF membranes (Sigma-Aldrich, St. Louis, MO, USA). The membranes were probed with primary antibodies against SMN/Gemin 1 (1:1000, ab108531, Abcam, Cambridge, UK) and β -Tubulin (1:1000, 2148S, Cell Signaling Technology, Danvers, MA, USA), followed by HRP-conjugated secondary antibodies (1:20,000, bs-0295G-HRP, Bioss, Beijing, China). The protein bands were visualized via an enhanced chemiluminescence (ECL) substrate (NCM Biotech, Jiangsu, China).

2.10 Immunofluorescence Staining

The cells were fixed with 4% paraformaldehyde and permeabilized with 0.25% Triton X-100. After being blocked with goat serum, the cells were incubated with primary antibodies against neuron-specific markers [NSE (1:200, Abcam, UK) and neurofilament (NF) (1:200, Cell Signaling Technology, USA)] overnight at 4 °C, followed by incubation with fluorescently labeled secondary antibodies [goat anti-rabbit IgG H&L/HRP (1:200, Bioss, China) and goat anti-mouse IgG H&L/HRP (Bioss, China)]. Nuclei were counterstained with DAPI, and images were captured via a fluorescence microscope.

2.11 Cell Viability and Apoptosis Assays

To evaluate whether the reduction in cell viability is attributed to an increase in apoptosis, we employed TUNEL fluorescence and Annexin V, which enabled us to compare the apoptotic rates among the different experimental groups.

Cell viability was assessed via the MTT assay (Beyotime, China), and apoptosis was measured via the TUNEL assay (Beyotime, China) and an Annexin V-FITC apoptosis detection kit (Beyotime, China) according to the manufacturers' instructions.

2.12 Statistical Analysis

The data were analyzed via GraphPad Prism 9.4.0 (GraphPad Software, LLC, Boston, MA, USA) and are presented as the means \pm SDs. Statistical differences between groups were evaluated via a t test or one-way ANOVA, with p < 0.05 considered statistically significant.



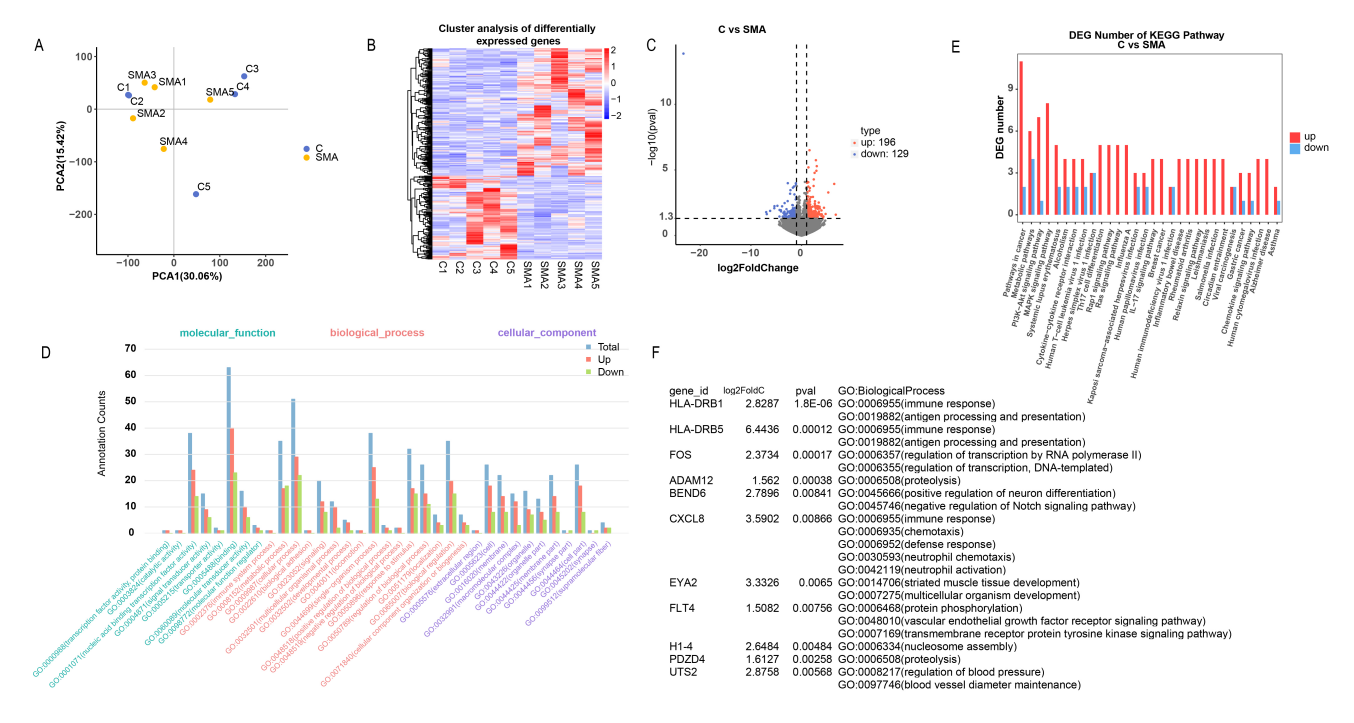


Fig. 1. Bioinformatics analysis of clinical samples. (A) Principal component analysis (PCA) plot showing the separation between the spinal muscular atrophy (SMA) and control groups. (B) Heatmap of differentially expressed genes (DEGs) differentiating the two groups. (C) Volcano plot indicating the number of upregulated and downregulated genes in the SMA group compared with the control group. (D,E) Gene Ontology (GO) and Kyoto Encyclopedia of Genes and Genomes (KEGG) enrichment analyses of the DEGs. (F) Selection of *UTS2* among the upregulated genes on the basis of stringent filtering criteria.

3. Results

3.1 Bioinformatics Analysis of Clinical Data

The principal component analysis (PCA) plot demonstrated distinct separation between the SMA and control groups, except for samples C1 and C2, which showed some overlap with the SMA group, indicating a unique transcriptional profile associated with SMA (Fig. 1A). The heatmap of differentially expressed genes (DEGs) further emphasized the difference between the two groups, highlighting that differential gene expression can serve as a robust classifier (Fig. 1B). Comparative analysis revealed 196 upregulated genes and 129 downregulated genes in the SMA group compared with the control group (Fig. 1C), suggesting a more pronounced effect of upregulated genes on SMA pathogenesis. The results indicated significant enrichment of upregulated genes in various biological processes and pathways (Fig. 1D,E), leading us to focus subsequent research on upregulated genes. The application of stringent criteria for gene selection based on a log2FoldChange greater than 1.5 and a p value \leq 0.01 resulted in the identification of 40 upregulated genes, among which HLA-DRB1, HLA-DRB5, FOS, ADAM12, BEND6, CXCL8, EYA2, FLT4, H1-4, PDZD4, and UTS2 were annotated with Gene Ontology Biological Process terms (Fig. 1F). Considering their potential relevance to the SMA context, UTS2 was selected for further investigation after a thorough literature review.

3.2 Reconstitution of the SMC Model

After the knockdown of *SMN1* in MSCs, we observed significant changes in cellular morphology and marker expression indicative of neuronal differentiation. The absence of CD34 expression and the presence of CD44 expression are associated with MSCs (Fig. 2A). Successful transfection was indicated by the positive signal of GFP (green fluorescent proteins) (Fig. 2B), while both the RNA (Fig. 2C) and protein (Fig. 2D) expression of SMN1 were significantly suppressed by shRNA.

After induction, the morphology of MSCs transformed into neuronal-like cells, characterized by cytoplasmic flattening and shrinkage toward the nucleus, as well as peripheral extension of cell membrane protrusions (Fig. 2E). Immunocytochemical staining confirmed the expression of neuron-specific markers, including neuronspecific enolase (NSE) and neurofilament (NF) proteins, in the differentiated cells (Fig. 2F). To assess the impact of SMN1 knockdown on the differentiation process, we measured the expression levels of SMN mRNA and protein in neuron-like cells via reverse transcription quantitative polymerase chain reaction (RT-qPCR) and Western blot methods, respectively. The results revealed a reduction in SMN expression postdifferentiation compared with preinduction levels, indicating that the knockdown effect was maintained throughout the differentiation process (Fig. 2G,H).



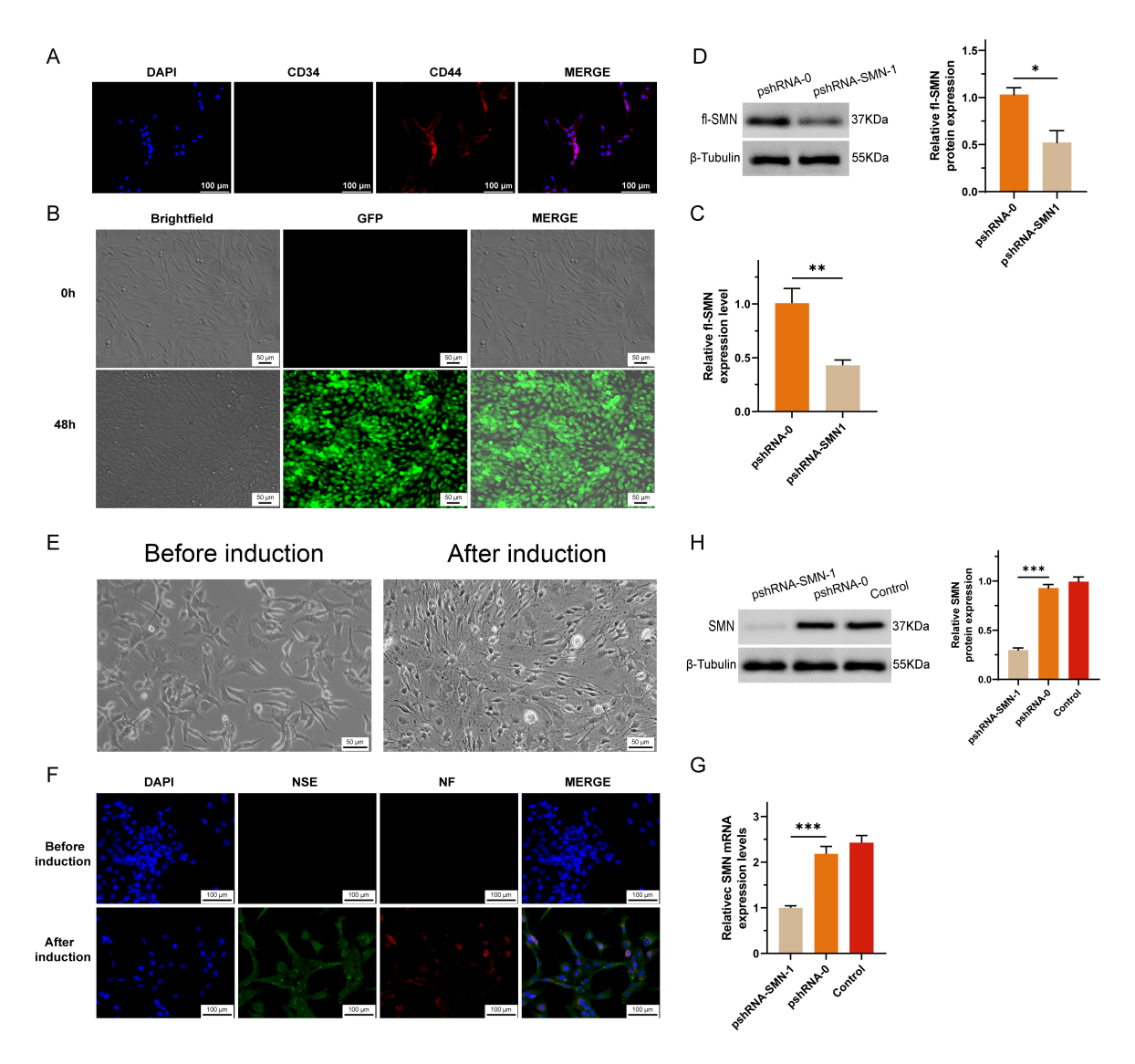


Fig. 2. Establishment and characterization of *SMN1* **knockdown in MSCs.** (A) Bone marrow was obtained from non-SMA patients, excluding those with concurrent blood diseases or bone tumors, to isolate and purify MSCs. (B) A short hairpin RNA (shRNA) construct targeting the survival motor neuron 1 (SMNI) gene was synthesized and cloned and inserted into a vector, creating a recombinant plasmid designed to express SMNI-shRNA within cells. (C,D) SMN1 knockdown in MSCs was evaluated by measuring SMN mRNA levels via RT-qPCR (C) and full-length SMN protein levels via Western blotting (D). A significant reduction in SMN expression confirmed the efficacy of the shRNA construct in silencing the SMNI gene. (E) Morphological changes indicative of neuronal differentiation in MSCs after infection with SMNI-targeting shRNA lentivirus. The images show that neurite outgrowth and changes in the cell body are characteristic of neuron-like cells. (F) Immunocytochemical staining confirming the expression of the neuron-specific markers NSE and NF in differentiated neuron-like cells, indicating successful differentiation. (G) RT-qPCR analysis demonstrating a sustained reduction in SMN mRNA levels in differentiated neuron-like cells compared with preinduction levels. (H) Western blot analysis showing decreased SMN protein expression in differentiated cells, which was consistent with the mRNA results and confirmed the maintenance of the SMNI knockdown effect. * represents p < 0.05, ** represents p < 0.01, and *** represents p < 0.001. The scale is 100 μm in (A) and (F) and 50 μm in (B) and (E). MSCs, mesenchymal stem cells; NSE, neuron-specific markers; NF, neurofilament; mRNA, messenger RNA; RT-PCR, transcription quantitative polymerase chain reaction.

3.3 Urantide Promotes Apoptosis in SMA Cell Models via the Caspase-3 Pathway

The cell survival curves revealed a positive proliferation trend in the SMA group, which was attenuated in a dose-dependent manner by urantide treatment, as observed

in the L-urrantide group and H-urrantide group (Fig. 3A). MTT assays corroborated these findings, revealing a significant decrease in cell viability with urantide treatment (Fig. 3B). TUNEL assays and flow cytometry via Annexin V staining revealed a significant increase in the number



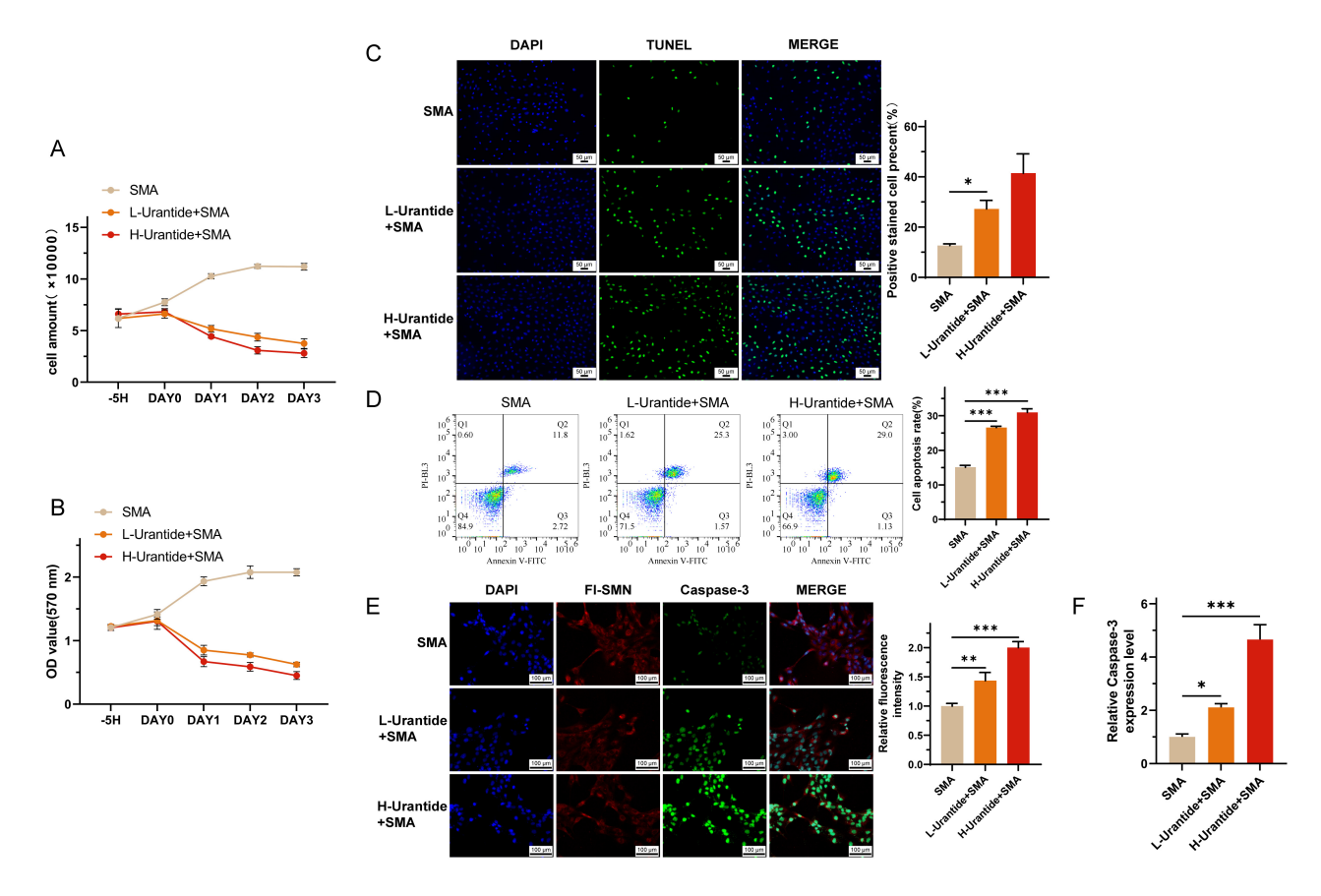


Fig. 3. Urantide-induced apoptosis in SMA cell models. (A) Cell survival curves depicting a dose-dependent attenuation of proliferation in SMA cells treated with urantide, as observed in the L-urrantide and H-urrantide groups. (B) MTT assays confirmed a significant decrease in cell viability with urantide treatment, indicating cytotoxic effects. (C) TUNEL fluorescence staining revealed a significant increase in apoptotic cells in response to urantide treatment, with higher concentrations leading to further increases in apoptosis rates. (D) Flow cytometry via Annexin V staining further demonstrated the proapoptotic effect of uride in a dose-dependent manner. (E) Immunofluorescence staining showing increased Caspase-3 protein expression in the urantide-treated groups, with the H-urrantide+SMA group exhibiting higher expression than the L-urrantide group and decreased SMN protein expression aligning with the mRNA levels. (F) RT-qPCR analysis confirming the upregulation of Caspase-3 mRNA in the urantide-treated groups, suggesting the activation of apoptotic pathways. * represents p < 0.05, ** represents p < 0.01, and *** represents p < 0.001. The scale is 50 μm in (C) and 100 μm in (E). MTT, 3-(4,5-dimethylthiazol-2-yl)-2,5-diphenyltetrazolium bromide; RT-qPCR, reverse transcription quantitative polymerase chain reaction.

of apoptotic cells in response to urantide treatment, with higher concentrations leading to further increases in apoptosis rates than those in the SMA group without intervention (Fig. 3C,D). RT-qPCR analysis revealed the upregulation of Caspase-3 mRNA in the urantide-treated groups, suggesting the induction of apoptotic pathways in the SMA cell model (Fig. 3F). Immunofluorescence staining revealed an increase in Caspase-3 protein expression in the urantide-treated groups, with higher expression observed in the H-urrantide+SMA group than in the L-urrantid group, and SMN protein expression was decreased in accordance with the mRNA levels (Fig. 3E).

4. Discussion

Our study presents significant findings that enhance the current understanding of SMA pathology. The identification of UTS2 as a highly expressed protein in SMA patients suggests its potential involvement in disease pathogenesis. The successful establishment of a stable MSC model with *SMN1* gene knockdown provides a valuable tool for investigating the effects of UTS2 inhibition. The observed effects of urantide on cell proliferation and apoptosis indicate a complex regulatory role of UTS2 in SMA-related cellular processes.

The development of a stable model for the knockdown of the *SMN1* gene in MSCs represents a significant advancement and provides a valuable resource for research on SMA. This model, which is specifically designed to reduce *SMN1* gene expression on the basis of existing SMA-derived induced pluripotent stem cell (iPSC) models [19], enables meticulous examination of the intricate interactions between UTS2 regulation and SMA pathophysiology. The



observed modulation of cell proliferation and apoptosis by the Urantide *UTS2* receptor antagonist further highlights the complex regulatory functions of *UTS2* in the SMA, demonstrating its multifaceted influence. By simulating key aspects of SMA pathology, this model serves as an important platform for exploring the therapeutic potential of UTS2 inhibition and advancing our understanding of the cellular dynamics in the SMA.

Our findings build upon the existing body of research that supports the neuroprotective role of *UTS2* in neuronal survival and synaptic plasticity [15–18,20]. With respect to spinal muscular atrophy (SMA), our study elucidates the intricate functions of *UTS2* in diverse contexts. Traditionally, *UTS2* is believed to contribute to cell survival; however, our findings indicate that the aberrant expression of *UTS2* in SMA patients' nerve cells is deleterious to human health. This observation does not contradict the established neuroprotective role of *UTS2* but rather enhances our comprehension of its involvement under distinct pathological conditions [21,22]

The observation that urantide treatment significantly influences cell proliferation in SMA cell models is particularly intriguing. This finding is consistent with previous studies that have implicated UTS2 in promoting cell division and vascularization in cancerous tissues [11,17,23-26]. The dual role of UTS2 in both neurodegenerative diseases and cancer highlights the complexity of its biological functions and suggests that targeted therapies must be carefully designed to address the specific pathological context [27– 29]. In conclusion, our study not only broadens the understanding of the role of UTS2 in the SMA but also underscores the need for a more comprehensive evaluation of its functions under different physiological and pathological conditions. The contrasting effects of UTS2 in SMAs versus its neuroprotective role in other contexts necessitate further investigation into the molecular mechanisms underlying these divergent outcomes. This knowledge is crucial for the development of targeted therapeutics that can effectively modulate *UTS2* activity in a disease-specific manner.

The observed increase in Caspase-3 expression following urantide treatment suggested that UTS2 may regulate apoptotic pathways in the SMA. This finding is consistent with the known role of *UTS2* in neuronal cell death [14] and suggests a potential mechanism by which *UTS2* contributes to SMA progression.

The significant biological effects of urrantide on the SMA cell model, including reduced cell viability and increased apoptosis, indicate its potential as a therapeutic agent. These results support the need for further investigations into UTS2 inhibitors as novel treatment strategies for SMA, which may lead to improved clinical management. While our study provides valuable insights into the role of UTS2 in SMAs, it is not without limitations. First, the *in vitro* nature of the experiments limits the extrapolation of these findings to the *in vivo* context, and the relatively small

sample size consisting of only five SMA patients and five controls for bioinformatics analysis may limit the generalizability of our findings and introduce potential sampling bias. Second, while our study emphasized Caspase-3 upregulation posturrantide treatment as a marker of apoptosis, we recognize the importance of exploring alternative apoptosis pathways and potential off-target effects. Third, concerning the dose-dependent effects of urantide, we acknowledge the absence of toxicity studies and the impact of urantide on non-SMA cells, which currently limits the therapeutic applicability of our findings. Future research should focus on in vivo models and need to be validated in larger cohorts to confirm the therapeutic potential of uride and explore its long-term effects on SMA progression; investigate additional apoptotic pathways beyond Caspase-3, including those involving Caspase-9 and Caspase-8, to comprehensively understand the cell death mechanisms influenced by uride; assess the toxicity and off-target effects of urantide, especially in non-SMA cells, to fully evaluate its safety profile and therapeutic index; and expand the sample size to increase the statistical robustness and generalizability of the findings.

5. Conclusion

Our study elucidates the role of *UTS2* in SMA and identifies UTS2 as a potential therapeutic target. The use of urantide to modulate the SMA cellular phenotype presents a promising avenue for future research and clinical development. Further studies are warranted to fully understand the mechanisms by which *UTS2* influences the SMA and to harness this knowledge for the benefit of patients.

Availability of Data and Materials

The data used and/or analyzed during the current study are available from the corresponding author on reasonable request.

Author Contributions

Conceptualization: XZ; Data curation: XZ; Formal analysis: LQY; Investigation: LQY; Writing—original draft: XZ. Both authors contributed to editorial changes in the manuscript. Both authors read and approved the final manuscript. Both authors have participated sufficiently in the work and agreed to be accountable for all aspects of the work.

Ethics Approval and Consent to Participate

The study was approved by the Fuyang People's Hospital ethics committee (approval number: [2024]64), and all patients or their families/legal guardians provided informed consent in accordance with the ethical standards of the Helsinki declaration.



Acknowledgment

The authors express their appreciation to staff in the second affiliated hospital of Anhui Medical University for their technical assistance.

Funding

This research was funded by the health research project of Fuyang Health Commission (grant number: FY2023-141).

Conflict of Interest

The authors declare no conflict of interest.

References

- Ogino S, Leonard DGB, Rennert H, Ewens WJ, Wilson RB. Genetic risk assessment in carrier testing for spinal muscular atrophy. American Journal of Medical Genetics. 2002; 110: 301–307. https://doi.org/10.1002/ajmg.10425.
- [2] Pearn J. Incidence, prevalence, and gene frequency studies of chronic childhood spinal muscular atrophy. Journal of Medical Genetics. 1978; 15: 409–413. https://doi.org/10.1136/jmg.15.6.
- [3] Sugarman EA, Nagan N, Zhu H, Akmaev VR, Zhou Z, Rohlfs EM, et al. Pan-ethnic carrier screening and prenatal diagnosis for spinal muscular atrophy: clinical laboratory analysis of >72,400 specimens. European Journal of Human Genetics. 2012; 20: 27–32. https://doi.org/10.1038/ejhg.2011.134.
- [4] Lefebvre S, Bürglen L, Reboullet S, Clermont O, Burlet P, Viollet L, *et al.* Identification and characterization of a spinal muscular atrophy-determining gene. Cell. 1995; 80: 155–165. https://doi.org/10.1016/0092-8674(95)90460-3.
- [5] Spinal muscular atrophy. Nature Reviews Disease Primers. 2022; 8: 51. https://doi.org/10.1038/s41572-022-00385-3.
- [6] Kim JK, Jha NN, Awano T, Caine C, Gollapalli K, Welby E, et al. A spinal muscular atrophy modifier implicates the SMN protein in SNARE complex assembly at neuromuscular synapses. Neuron. 2023; 111: 1423–1439.e4. https://doi.org/10.1016/j.neuron.2023.02.004.
- [7] Monani UR. Spinal muscular atrophy: a deficiency in a ubiquitous protein; a motor neuron-specific disease. Neuron. 2005; 48: 885–896. https://doi.org/10.1016/j.neuron.2005.12.001.
- [8] Mendell JR, Al-Zaidy S, Shell R, Arnold WD, Rodino-Klapac LR, Prior TW, et al. Single-Dose Gene-Replacement Therapy for Spinal Muscular Atrophy. The New England Journal of Medicine. 2017; 377: 1713–1722. https://doi.org/10.1056/NE JMoa1706198.
- [9] Finkel RS, Mercuri E, Darras BT, Connolly AM, Kuntz NL, Kirschner J, et al. Nusinersen versus Sham Control in Infantile-Onset Spinal Muscular Atrophy. The New England Journal of Medicine. 2017; 377: 1723–1732. https://doi.org/10.1056/NE JMoa1702752.
- [10] Sivaramakrishnan M, McCarthy KD, Campagne S, Huber S, Meier S, Augustin A, et al. Binding to SMN2 pre-mRNAprotein complex elicits specificity for small molecule splicing modifiers. Nature Communications. 2017; 8: 1476. https://doi. org/10.1038/s41467-017-01559-4.
- [11] Yanfei W, Langping S, Mingzhong S. Prognostic Significance and Functional Mechanism of UTS2 in Glioblastoma Multiforme. Current Cancer Drug Targets. 2024. https://doi.org/10. 2174/0115680096275291231226081320. (in press)
- [12] Kwok T, Huerta-White T, Briegel K, Singh A, Yeguvapalli S, Chitrala KN. Bioinformatics analysis of the potential biomark-

- ers of Multiple Sclerosis and Guillain—Barré syndrome. 2024. bioRxiv. https://doi.org/10.1101/2024.05.29.595759. (preprint)
- [13] de Miguel-Gómez L, Sebastián-León P, Romeu M, Pellicer N, Faus A, Pellicer A, et al. Endometrial gene expression differences in women with coronavirus disease 2019. Fertility and Sterility. 2022; 118: 1159–1169. https://doi.org/10.1016/j.fertnstert.2022.09.013.
- [14] Deng Z, Liu J, He S, Gao W. The Pyroptosis-Related Signature Predicts Diagnosis and Indicates Immune Characteristic in Major Depressive Disorder. Frontiers in Pharmacology. 2022; 13: 848939. https://doi.org/10.3389/fphar.2022.848939.
- [15] Quan FB, Gaillard AL, Alejevski F, Pézeron G, Tostivint H. Urotensin II-related peptide (Urp) is expressed in motoneurons in zebrafish, but is dispensable for locomotion in larva. Peptides. 2021; 146: 170675. https://doi.org/10.1016/j.peptides.2021.170675.
- [16] Bearce EA, Irons ZH, O'Hara-Smith JR, Kuhns CJ, Fisher SI, Crow WE, et al. Urotensin II-related peptides, Urp1 and Urp2, control zebrafish spine morphology. 2022; 11: e83883. https://doi.org/10.7554/eLife.83883.
- [17] Dubessy C, Cartier D, Lectez B, Bucharles C, Chartrel N, Montero-Hadjadje M, et al. Characterization of urotensin II, distribution of urotensin II, urotensin II-related peptide and UT receptor mRNAs in mouse: evidence of urotensin II at the neuromuscular junction. Journal of Neurochemistry. 2008; 107: 361–374. https://doi.org/10.1111/j.1471-4159.2008.05624.x.
- [18] Vaudry H, Do Rego J-C, Le Mevel J-C, Chatenet D, Tostivint H, Fournier A, *et al.* Urotensin II, from fish to human. Annals of the New York Academy of Sciences. 2010; 1200: 53–66. https://doi.org/10.1111/j.1749-6632.2010.05514.x.
- [19] Zeng W, Kong X, Alamana C, Liu Y, Guzman J, Pang PD, et al. Generation of two induced pluripotent stem cell lines from spinal muscular atrophy type 1 patients carrying no functional copies of SMN1 gene. Stem Cell Research. 2023; 69: 103095. https://doi.org/10.1016/j.scr.2023.103095.
- [20] Vaudry H, Leprince J, Chatenet D, Fournier A, Lambert DG, Le Mével JC, et al. International Union of Basic and Clinical Pharmacology. XCII. Urotensin II, urotensin II-related peptide, and their receptor: from structure to function. Pharmacological Reviews. 2015; 67: 214–258. https://doi.org/10.1124/pr .114.009480.
- [21] Fraser DR. Emerging roles of urotensin-II in cardiovascular disease. Pharmacology & Therapeutics. 2004; 103: 223–243. https://doi.org/10.1016/j.pharmthera.2004.07.004.
- [22] Ogbonmide T, Rathore R, Rangrej SB, Hutchinson S, Lewis M, Ojilere S, et al. Gene Therapy for Spinal Muscular Atrophy (SMA): A Review of Current Challenges and Safety Considerations for Onasemnogene Abeparvovec (Zolgensma). Cureus. 2023; 15: e36197. https://doi.org/10.7759/cureus.36197.
- [23] Pereira-Castro J, Brás-Silva C, Fontes-Sousa AP. Novel insights into the role of urotensin II in cardiovascular disease. Drug Discovery Today. 2019; 24: 2170–2180. https://doi.org/10.1016/j. drudis.2019.08.005.
- [24] Sun S, Liu L. Urotensin II: an inflammatory cytokine. Journal of Endocrinology. 2019; 204: R107–R117. https://doi.org/10. 1530/joe-18-0505.
- [25] Svistunov AA, Tarasov VV, Shakhmardanova SA, Sologova SS, Bagaturiya ET, Chubarev VN, et al. Urotensin II: molecular mechanisms of biological activity. Current Protein and Peptide Science. 2018; 19: 924–934. https://doi.org/10.2174/1389203718666170829162335.
- [26] Yumrutas O, Oztuzcu S, Büyükhatipoglu H, Bozgeyik I, Bozgeyik E, Igci YZ, et al. The role of the UTS2 gene polymorphisms and plasma Urotensin-II levels in breast cancer. Tumor Biology. 2015; 36: 4427–4432. https://doi.org/10.1007/s13277-015-3082-2.
- [27] Hirose T, Takahashi K, Mori N, Nakayama T, Kikuya M,



- Ohkubo T, et al. Increased expression of urotensin II, urotensin II-related peptide and urotensin II receptor mRNAs in the cardiovascular organs of hypertensive rats: comparison with endothelin-1. Peptides. 2009; 30: 1124–1129. https://doi.org/10.1016/j.peptides.2009.02.009.
- [28] Jarry M, Diallo M, Lecointre C, Desrues L, Tokay T, Chatenet D, *et al.* The vasoactive peptides urotensin II and urotensin II-
- related peptide regulate astrocyte activity through common and distinct mechanisms: involvement in cell proliferation. The Biochemical Journal. 2010; 428: 113–124. https://doi.org/10.1042/BJ20090867.
- [29] Langham RG, Kelly DJ. Urotensin II and the kidney. Current Opinion in Nephrology and Hypertension. 2013; 22: 107–112.

